

Universal quantum computation with electronic qubits in decoherence-free subspace

X.L. Zhang^{1,2,*}, M. Feng^{1,†} and K.L. Gao^{1‡}

¹*State Key Laboratory of Magnetic Resonance and Atomic and Molecular Physics,*

Wuhan Institute of Physics and Mathematics,

Chinese Academy of Sciences, Wuhan 430071, China and

²*Graduate School of the Chinese Academy of Sciences, Beijing 100049, China*

We investigate how to carry out universal quantum computation deterministically with free electrons in decoherence-free subspace by using polarizing beam splitters, charge detectors, and single-spin rotations. Quantum information in our case is encoded in spin degrees of freedom of the electron-pairs which construct a decoherence-free subspace. We design building blocks for two noncommutable single-logic-qubit gates and a logic controlled phase gate, based on which a universal and scalable quantum information processing robust to dephasing is available in a deterministic way.

PACS numbers: 03.67.Lx, 03.67.Pp, 03.67.Mn

I. INTRODUCTION

Decoherence is one of the main obstacles in building quantum computing architecture, which yields both operational errors and loss of coherence and entanglement. To defeat decoherence, people have so far proposed a number of ideas, for example in [1, 2, 3, 4, 5, 6, 7, 8], where the error avoiding strategies carried out in decoherence-free subspaces (DFS), compared with other error correction schemes, are relatively simpler, because they only require some special encodings immune from certain system-environment disturbances and no error correction steps are needed.

The present work is focused on a dephasing-free scheme for universal quantum computation with free electrons. Free electrons have recently been shown to be available for constructing universal quantum computation [9, 10], in which the basic idea is the quantum information encoded in electron spins and the quantum gating assisted by electronic charge detection. Due to indepen-

*xlzhang168@gmail.com; present address: Center for Modern Physics and Department of Physics, Chongqing University, Chongqing 400044, China

†mangfeng1968@yahoo.com

‡klgao@wipm.ac.cn

dence between the spin and charge degrees of freedom of the electrons, we may design a quantum computing architecture with free electrons like the idea used in linear optical quantum computation [11]. For example, like photons, electrons could be employed to carry out cluster-state preparation and multipartite analyzer [12], and to do entanglement purification [13]. But actually, there are some intrinsic differences between electrons and photons. The photons do not interact directly with each other, but electrons repel due to Coulomb interaction. So the works [9, 10] are based on a screening model in which interaction-free assumption is applicable to free electrons. Besides, different polarized states are degenerate to photons, which excludes any possibility of dephasing due to different states in evolution. While an electronic level would be split in a magnetic field due to Zeeman interaction. As a result, dephasing is an important detrimental factor in application of free electrons for quantum computation.

To remove dephasing effects, we used to employ refocusing techniques, which reverse the time evolution during some elaborately selected periods, and counteract the influence from dephasing. However, refocusing operation does not work for magnetic field fluctuation, which happens unpredictably in experiments. To reduce dephasing, we must work in DFS. *The motivation of this paper is to design a DFS scheme for free-electron model so that the free electrons, in addition to above mentioned screening assumption, could be fully modeled as free photons for quantum computation.* We define the encoding to be $|0_L\rangle = |01\rangle$ and $|1_L\rangle = |10\rangle$, which constitutes a well-known DFS scheme immune from dephasing induced by the system-environment interaction in the form of $Z \otimes B$, where $Z = \sigma_z^1 \oplus \sigma_z^2$ and B is a random bath operator. We will assume throughout our scheme that the collective dephasing is dominant for the electron pairs because the collective errors due to coupling to environment are generally considered to be the main problem for solid-state systems at low temperature and dephasing is dominant in the corresponding class of quantum computing devices. While for other dephasing effects, we may overcome them with the same DFS encoding by some additional dynamical decoupling (e.g., 'Bang-Bang') pulses [14, 15]. To avoid confusion, we call $|0_L\rangle$ and $|1_L\rangle$ logic-qubits, and $|0\rangle$ and $|1\rangle$ physical-qubits with 0 (1) representing spin up (down). The four Bell states in our scheme are thereby expressed as $|\Psi_L^\pm\rangle = (|0110\rangle \pm |1001\rangle)/\sqrt{2} \equiv (|0_L1_L\rangle \pm |1_L0_L\rangle)/\sqrt{2}$ and $|\Phi_L^\pm\rangle = (|0101\rangle \pm |1010\rangle)/\sqrt{2} \equiv (|0_L0_L\rangle \pm |1_L1_L\rangle)/\sqrt{2}$. Since the logic-qubits are immune from collective dephasing, the dephasing errors would be considerably suppressed in implementation of our designed quantum computation.

II. BUILDING BLOCKS FOR QUANTUM GATES

We now address in detail how to realize a universal quantum computation in the DFS by building blocks involving polarizing beam splitters, charge detectors, and single-spin rotations. The basic components for a universal quantum computation are two noncommutable single-qubit operations and a nontrivial two-qubit gate. For an arbitrary logic-qubit state, e.g., $\alpha|0_L\rangle + \beta|1_L\rangle \equiv \alpha|01\rangle + \beta|10\rangle$, a single-logic-qubit rotation R_z can be realized by rotating one of the physical-qubits, as shown in Fig. 1 (a): If we consider a rotation of the first physical-qubit, as the potential barrier in Fig. 1 (a) makes $|1\rangle$ be $e^{i\theta}|1\rangle$ but $|0\rangle$ unchanged, we have $\alpha|0_L\rangle + \beta|1_L\rangle \Rightarrow \alpha|01\rangle + \beta e^{i\theta}|10\rangle = \alpha|0_L\rangle + \beta e^{i\theta}|1_L\rangle$, where the phase θ is determined by the characteristic of the potential barrier. Besides its own function in universal quantum computation, this rotation gate R_z will be also used below for achieving other gates.

Another important single-logic-qubit gate is Hadamard gate, i.e.,

$$\alpha|0_L\rangle + \beta|1_L\rangle \rightarrow [\alpha(|0_L\rangle + |1_L\rangle) + \beta(|0_L\rangle - |1_L\rangle)]/\sqrt{2}, \quad (1)$$

with α and β arbitrary numbers, and $\alpha^2 + \beta^2 = 1$. To do this job in DFS, we have to introduce ancillary physical-qubits $1'$ and $2'$ which are initially prepared in $(|01\rangle_{1'2'} + |10\rangle_{1'2'})/\sqrt{2}$. As shown in the inset of Fig. 2, the initial state $(|01\rangle_{1'2'} + |10\rangle_{1'2'})/\sqrt{2}$ can be made in the case of $P_{1'2'}=0$, where $P_{1'2'}$ is a charge parity measurement building block designed in Fig. 2 of [9]. $P_{1'2'}$ functions as: $P=1$ means the two input spins aligned, and $P=0$ corresponds to the opposite spins input. So we have the initial state of the system as

$$\begin{aligned} |\Psi\rangle &= (\alpha|0_L\rangle + \beta|1_L\rangle)_{12} \otimes (|01\rangle_{1'2'} + |10\rangle_{1'2'})/\sqrt{2} \\ &= [\alpha(|0101\rangle_{121'2'} + |0110\rangle_{121'2'}) + \beta(|1001\rangle_{121'2'} + |1010\rangle_{121'2'})]/\sqrt{2}. \end{aligned}$$

Besides the ancillary qubits, a controlled-phase operation between physical-qubits 1 and $1'$ is necessary in constructing our Hadamard gate for logic-qubits, which is shown in Appendix and also in Fig. 1(b). After this controlled-phase gate is applied, we have

$$|\Psi'\rangle = [\alpha(|0101\rangle_{121'2'} + |0110\rangle_{121'2'}) + \beta(|1001\rangle_{121'2'} - |1010\rangle_{121'2'})]/\sqrt{2}. \quad (2)$$

Then if we find in Fig. 2 that $D_1 = 1$ and $D_2 = 0$, which implies that input physical-qubits are in a state $(|01\rangle + |10\rangle)/\sqrt{2}$ [9], then the qubit pair $1'-2'$ collapses to

$$\alpha(|01\rangle_{1'2'} + |10\rangle_{1'2'})/\sqrt{2} + \beta(|01\rangle_{1'2'} - |10\rangle_{1'2'})/\sqrt{2},$$

which is exactly a Hadamard gate for logic-qubits in DFS but with the quantum information transferred from pair 1-2 to pair 1'-2'. This trick has also been used previously for neutral atoms in DFS [8]. We may have an alternative for the last step, that is, in the case of $D_1 = 0$ and $D_2 = 1$, the qubit pair 1'-2' collapses to

$$\alpha (|01\rangle_{1'2'} + |10\rangle_{1'2'})/\sqrt{2} - \beta (|01\rangle_{1'2'} - |10\rangle_{1'2'})/\sqrt{2}.$$

For this situation, we may also have our desired Hadamard gate after additional spin-flip σ_x operations are applied on physical-qubits 1' and 2', respectively. Therefore we have achieved a logic-qubit Hadamard gate deterministically by four physical-qubits with quantum information transferred from the pair 1-2 to the pair 1'-2', i.e., $|0_L\rangle_{12} \Rightarrow (|0_L\rangle_{1'2'} + |1_L\rangle_{1'2'})/\sqrt{2}$ and $|1_L\rangle_{12} \Rightarrow (|0_L\rangle_{1'2'} - |1_L\rangle_{1'2'})/\sqrt{2}$.

To accomplish a universal quantum computation, however, we also need a nontrivial two-logic-qubit gate. Fig. 3 demonstrates a controlled-phase gate for two logic-qubits consisting of pairs 1-2 and 5-6, assisted by an ancillary pair 3-4 which are measured at the end of the circuit. So the total system is initially prepared in

$$|\Phi\rangle = (\alpha |01\rangle_{12} + \beta |10\rangle_{12}) \otimes (|01\rangle_{34} + |10\rangle_{34})/\sqrt{2} \otimes (c |01\rangle_{56} + d |10\rangle_{56}), \quad (3)$$

where α, β, c and d are arbitrary numbers with $\alpha^2 + \beta^2 = 1$ and $c^2 + d^2 = 1$. After we have the charge detection at P_{13} with $P_{13} = 1$, the system becomes

$$(\alpha |0101\rangle_{1234} + \beta |1010\rangle_{1234}) \otimes (c |01\rangle_{56} + d |10\rangle_{56}), \quad (4)$$

where the first four qubits are entangled as a Bell state of the logic-qubits when $\alpha = \beta = 1/\sqrt{2}$. Please note that, if $P_{13} = 0$, the system are still in the DFS, i.e.,

$$(\alpha |0110\rangle_{1234} + \beta |1001\rangle_{1234}) \otimes (c |01\rangle_{56} + d |10\rangle_{56}),$$

from which we may also achieve Eq. (4) by additional spin-flip operations σ_x on physical-qubits 3 and 4. Following the operation steps in Fig. 3, we have to twice use the Hadamard gate designed in Fig. 2, and go through a block P_{46} . In the case of $P_{46} = 1$, we obtain the output of the system,

$$\begin{aligned} |\Phi'\rangle = & (\alpha c |0101\rangle_{1256} + \alpha d |0110\rangle_{1256} + \beta c |1001\rangle_{1256} - \beta d |1010\rangle_{1256}) |01\rangle_{34} \\ & + (\alpha c |0101\rangle_{1256} - \alpha d |0110\rangle_{1256} + \beta c |1001\rangle_{1256} + \beta d |1010\rangle_{1256}) |10\rangle_{34}. \end{aligned} \quad (5)$$

So we measure the physical-qubits 3 and 4. The output $|01\rangle_{34}$ means a two-logic-qubit controlled phase gate to be achieved. Alternatively, if we have $|10\rangle_{34}$, the controlled phase gate is also available

after an additional operation $\sigma_z^5 \otimes I^6$ is applied on the pair 5-6. Moreover, if we find $P_{46} = 0$, the output should be in the state,

$$\begin{aligned} |\Phi'\rangle = & (\alpha c |0101\rangle_{1256} + \alpha d |0110\rangle_{1256} - \beta c |1001\rangle_{1256} + \beta d |1010\rangle_{1256}) |01\rangle_{34} \\ & + (-\alpha c |0101\rangle_{1256} + \alpha d |0110\rangle_{1256} + \beta c |1001\rangle_{1256} + \beta d |1010\rangle_{1256}) |10\rangle_{34}. \end{aligned} \quad (6)$$

Like previously, if the measurement on physical-qubits 3 and 4 yields $|01\rangle_{34}$ ($|10\rangle_{34}$), we may achieve the two-logic-qubit controlled phase gate after applying operation σ_z on physical-qubits 1 (1 and 5).

III. DISCUSSION

It was considered that quantum computation using free electrons is more powerful than using photons because the former is a deterministic one and thus needs less ancillary qubits [9]. Moreover, as the charge detection is non-destructive with respect to the qubits encoded in electron spins, there is no loss of qubits in the detection. As a result, we could have deterministic quantum gating by free electrons in the DFS, which is much more efficient than the probabilistic gating by photons. Furthermore, the ideas with photons - the flying qubits - interacting with static qubits (such as cold atoms or ions) are referred to as a promising way towards scalable quantum computation. While as the information conversion based on the interaction between photons and matter is generally inefficient, this kind of quantum computation, even in principle scalable, is of very low success rate. In contrast, the free electrons, for example, conduction electrons in solid-state materials, could play roles as both flying and static qubits, which would be a promising candidate for large-scale quantum computation [16].

Although the encoding with electron pairs by our scheme makes more than half numbers of qubits sacrificed, which increases overhead for quantum computation, the operation carried out in DFS much reduces the implementational time and difficulty, and enhances the fidelity. As seen in current experiments, refocusing pulses to remove dephasing have to be applied repeatedly even for a single quantum gating. In this sense, the sacrifice of qubit resource in our scheme helps saving time and laser pulses, and thereby increases the fidelity of implementation. In other words, with the encoding, we could treat free electrons with the same way as photons for a universal quantum computation. As our scheme could be done in a deterministic way, which is the prerequisite for a scalable quantum computation, the quantum computation with free electrons by our scheme could be more advantageous over the probabilistic ways by photons.

As mentioned previously, our focus is on the collective dephasing, which is supposed to be a dominant error due to magnetic field fluctuation and could be perfectly eliminated by our encoding. While there are also other errors beyond the collective dephasing one in a real quantum computation, such as logic errors regarding $\sigma_r^i \sigma_r^{i+1}$ with $r=x, y, z$, and the leakage errors related to following undesired operations: $\sigma_x^i, \sigma_x^{i+1}, \sigma_y^i, \sigma_y^{i+1}, \sigma_x^i \sigma_z^{i+1}, \sigma_z^i \sigma_x^{i+1}, \sigma_y^i \sigma_z^{i+1}, \sigma_z^i \sigma_y^{i+1}$ [14]. To eliminate the logic errors, we may employ deliberately designed pulse sequences including $\sigma_x^i \sigma_x^{i+1}, \sigma_y^i \sigma_y^{i+1}$, and $\sigma_z^i \sigma_z^{i+1}$ respectively. As this implementation might be not fast enough, however, the 'Bang-Bang' pulse control would not fully remove the logic errors, which need further amendment by refocusing on individual physical-qubits [14]. The leakage errors could be in principle fully removed by the leakage-elimination operator introduced by [15]. This operator is actually associated with projection operations which could be applied to our free electron case. Moreover, since the errors are brought about by unpredictable factors, e.g., the fluctuation of the magnetic field, we have to first use interrogative 'Bang-Bang' pulses to determine the required values for correction, which has been actually a sophisticated technique [17]. A very recent experiment [18] with two-dimensional electron gas made of GaAs/AlGaAs heterostructure has successfully extended T_2 from 10 nanosec to 1 microsec by using the 'Bang-Bang' pulses. So, with the encoding plus 'Bang-Bang' pulses assisted sometimes by individual physical-qubit refocusing, all dephasing errors could be strongly suppressed in our free-electron quantum computation [14].

Besides dephasing, however, there are other sources of decoherence to affect free electrons, e.g., the decoherence yielding T_1 . Fortunately, as reported in [19], T_1 could be extended from microsec to tens of millisecc in systems of two-dimensional electron gas by means of 'Bang-Bang' pulses. This spin relaxing time is long enough for us to achieve high-quality quantum information processing.

The beam splitters and charge detectors employed in our scheme have been experimentally achieved by means of the point contacts in a two-dimensional electron gas [20, 21, 22, 23]. From the experimental values, we may estimate that each beam splitter takes hundreds of nanosec for an electronic parity check [20, 21] and each Hadamard gate also takes hundreds of nanosec [24]. Moreover, the currently achievable time resolution for charge detection is of the order of *microsec* [21]. So considering all the operations in the gates designed in the present paper, the time we have to take would be of the order of microsec, which is much shorter than the above mentioned T_1 . With the advance of techniques, we believe that this time would be further reduced in the near future. For example, it is expected that the time resolved detection required in charge detector for the ballistic electrons in a semiconductor will be in the *pico*sec range [9, 25]. Compared to previous proposals for electron-spin-based quantum computation, e.g., the famous one [26] in which the qubits are

encoded in the spin of the single access electron in conduction band of semiconductor quantum dots and the two-qubit gate is carried out by exchange interaction in the interdot tunneling, our scheme is not more stringent in implementation. Particularly, as T_2 is much longer in our scheme with DFS encoding, we could achieve a quantum computation with higher fidelity than by any previous scheme without the DFS encoding. Furthermore, as our proposal is for free electrons, our idea could be applied to the spin-based quantum computing proposal for the electrons floating on liquid Helium [27].

On the other hand, since the charge detectors in our scheme function to distinguish the antiparallel states of two electron-spin from the parallel states, we may consider an alternative way, as reported in [10], to convert spin parity into charge information by resonant tunneling between two quantum dots. With this resonant tunneling characteristic, one can determine the parity of two-qubit spins by differentiating the spin states with antiparallel spins from the ones with parallel spins, in which quantum information encoded in the spin qubits is not destroyed.

IV. CONCLUSION AND ACKNOWLEDGMENTS

In summary, we have proposed a potential scheme for universal quantum computation with free electrons in DFS in a deterministic way by using polarizing beam splitters, charge detectors, and single-spin rotations. Two noncommutable single-logic-qubit gates, i.e., R_z operation and Hadamard gate, and a two-logic-qubit controlled phase gate have been designed and demonstrated. With these building blocks, an universal dephasing-free quantum computing architecture can be constructed for free electrons.

This work is supported in part by National Natural Science Foundation of China under Grant Nos. 10474118 and 60490280, by Hubei Provincial Funding for Distinguished Young Scholars, and by the National Fundamental Research Program of China under Grant No. 2005CB724502 and No. 2006CB921203.

V. REFERENCES

-
- [1] G. M. Palma, K. -A. Suominen, A. K. Ekert (1996), *Quantum Computers and Dissipation*, Proc. R. Soc. London A 452, 567-584.

- [2] L. -M. Duan and G. -C. Guo (1997), *Preserving Coherence in Quantum Computation by Pairing Quantum Bits*, Phys. Rev. Lett., 79, pp. 1953-1956; P. Zanardi and M. Rasetti (1997), *Noiseless Quantum Codes*, Phys. Rev. Lett., 79, 3306-3309.
- [3] D. A. Lidar, I. L. Chuang, and K. B. Whaley (1998), *Decoherence-Free Subspaces for Quantum Computation*, Phys. Rev. Lett., 81, 2594-2597.
- [4] J. Kempe, D. Bacon, D. A. Lidar, and K. B. Whaley (2001), *Theory of decoherence-free fault-tolerant universal quantum computation*, Phys. Rev. A, 63, pp. 042307-1-042307-29; D. A. Lidar, D. Bacon, J. Kempe, and K. B. Whaley (2001), *Decoherence-free subspaces for multiple-qubit errors: II. Universal, fault-tolerant quantum computation*, Phys. Rev. A, 63, pp. 022307-1-022307-18.
- [5] D. A. Lidar and L. -A. Wu (2003), *Encoded recoupling and decoupling: An alternative to quantum error-correcting codes applied to trapped-ion quantum computation*, Phys. Rev. A, 67, pp. 022313-1-022313-12.
- [6] W. Y. Hwang, H. Lee, D. Ahn, and S. W. Hwang (2000), *Efficient schemes for reducing imperfect collective decoherences*, Phys. Rev. A, 62, pp. 0062305-1-062305-3.
- [7] L. -A. Wu, P. Zanardi, and D. A. Lidar (2005), *Holonomic Quantum Computation in Decoherence-Free Subspaces*, Phys. Rev. Lett., 95, pp. 130501-1-130501-4.
- [8] P. Xue and Y.-F. Xiao (2006), *Universal Quantum Computation in Decoherence-Free Subspace with Neutral Atoms*, Phys. Rev. Lett., 97, pp. 140501-1-140501-4.
- [9] C. W. J. Beenakker, D. P. DiVincenzo, C. Emary, and M. Kindermann (2004), *Charge Detection Enables Free-Electron Quantum Computation*, Phys. Rev. Lett., 93, pp. 020501-1-020501-4.
- [10] H. A. Engel and D. Loss (2005), *Fermionic Bell-State Analyzer for Spin Qubits*, Science, 309, pp. 586-588.
- [11] E. Knill, R. Laflamme, and G. J. Milburn (2001), *A scheme for efficient quantum computation with linear optics*, Nature (London), 409, pp. 46-62.
- [12] X. L. Zhang, M. Feng, and K. L. Gao (2006), *Cluster-state preparation and multipartite entanglement analyzer with fermions*, Phys. Rev. A, 73, pp. 014301-1-014301-4.
- [13] X. -L. Feng, L. C. Kwek, and C. H. Oh (2005), *Electronic entanglement purification scheme enhanced by charge detections*, Phys. Rev. A, 71, pp. 064301-1-064301-3.
- [14] M. S. Byrd and D. A. Lidar (2002), *Comprehensive Encoding and Decoupling Solution to Problems of Decoherence and Design in Solid-State Quantum Computing*, Phys. Rev. Lett., 89, pp. 047901-1-047901-4.
- [15] L. -A. Wu, M. S. Byrd, and D. A. Lidar (2002), *Efficient Universal Leakage Elimination for Physical and Encoded Qubits*, Phys. Rev. Lett., 89, pp. 127901-1-127901-4.
- [16] We mean the scalability here by the fact that a universal quantum computation could be built by a series of two noncommutable single-qubit operations and nontrivial two-qubit gates. As we have constructed these component gates in DFS encoding, a large-scale dephasing-free quantum computation could work. This is different from the multi-qubit DFS encoding under strong and fast 'Bang-Bang' pulses, e.g., by

- L.-A. Wu and D.A. Lindar in Phys. Rev. Lett. 88, 207902 (2002).
- [17] L. M. K. Vandersypen and I. L. Chuang (2004), *NMR techniques for quantum control and computation*, Rev. Mod. Phys. 76, pp 1037-1069.
 - [18] J. R. Petta, A. C. Johnson, J. M. Taylor, E. A. Laird, A. Yacoby, M. D. Lukin, C. M. Marcus, M. P. Hanson and A. C. Gossard A C (2007), *Coherent manipulation of coupled electron spins in semiconductor quantum dots*, Science 309, pp. 2180-2184.
 - [19] A. C. Johnson, J. R. Petta, J. M. Taylor, A. Yacoby, M. D. Lukin, C. M. Marcus, M. P. Hanson, and A. C. Gossard (2005), *Triplet-singlet spin relaxation via nuclei in a double quantum dot*, Nature (London), 435, pp. 925-928.
 - [20] M. Henny, S. Oberholzer, C. Strunk, T. Heinzel, K. Ensslin, M. Holland, C. Schönenberger (1999), *The Fermionic Hanbury Brown and Twiss Experiment*, Science, 284, pp. 296-298.
 - [21] W. D. Oliver, J. Kim, R. C. Liu, Y. Yamamoto (1999), *Hanbury Brown and Twiss-Type Experiment with Electrons*, Science, 284, pp. 299-301.
 - [22] E. Buks, R. Schuster, M. Heiblum, D. Mahalu, and V. Umansky (1998), *Dephasing in electron interference by a 'which-path' detector*, Nature (London), 391, pp. 871-874.
 - [23] J. M. Elzerman, R. Hanson, L. H. Willems van Beveren, L. M. K. Vandersypen, and L. P. Kouwenhoven (2004), *Excited-state spectroscopy on a nearly closed quantum dot via charge detection*, Appl. Phys. Lett., 84, pp. 4617-4619.
 - [24] F. H. L. Koppens, C. Buizert, K. J. Tielrooij, I. T. Vink, K. C. Nowack, T. Meunier, L. P. Kouwenhoven and L. M. K. Vandersypen (2006), *Driven coherent oscillations of a single electron spin in a quantum dot*, Nature (London), 442, pp. 766-771.
 - [25] E. A. Shaner and S. A. Lyon (2004), *Picosecond Time-Resolved Two-Dimensional Ballistic Electron Transport*, Phys. Rev. Lett., 93, pp. 037402-1-037402-4.
 - [26] D. Loss and D.P. DiVincenzo (1998), *Quantum computation with quantum dots*, Phys. Rev. A, 57, pp. 120-126.
 - [27] S. A. Lyon (2006), *Spin-based quantum computing using electrons on liquid Helium*, Phys. Rev. A, 74, pp. 052338-1-052338-6.

Captions of the figures

Fig. 1 (a) The schematic for a rotation gate R_z , where one of the two physical-qubits in a pair experiences a potential barrier. Due to level splitting, the electron with spin-down will get a phase θ after tunneling the potential barrier, while the electron with spin-up remains unchanged. So an electron in superposition of $|\uparrow\rangle$ and $|\downarrow\rangle$ will turn to that of $|\uparrow\rangle$ and $e^{i\theta}|\downarrow\rangle$ after getting through the potential barrier; (b) A controlled-phase gate on two physical-qubits input from control-in and target-in ports, where P_1 and P_2 are the charge parity measurement building blocks designed in Fig. 2 of [9], and H means a Hadamard gate on a physical-qubit. Two R_z operations are introduced for removing the undesired relative phases, as demonstrated in Appendix.

Fig. 2 Hadamard gate on logic-qubits in the DFS, where the dashed horizontal lines are two 50/50 beam splitters and the solid horizontal lines are two mirrors. σ_z is a local spin phase flip on the physical-qubit in that path. The charge detectors D_1 and D_2 operate as parity meters to single out the spin singlet state when $D_1=0$. The Hadamard gate of this kind makes $|01\rangle_{12} \Rightarrow (|01\rangle_{1'2'} + |10\rangle_{1'2'})/\sqrt{2}$ and $|10\rangle_{12} \Rightarrow (|01\rangle_{1'2'} - |10\rangle_{1'2'})/\sqrt{2}$. The inset accounts for preparing the initial state of physical-qubits $1'$ and $2'$: Suppose the input qubits are prepared in the state $|00\rangle$ (i.e., spin $|\uparrow\uparrow\rangle$), we can get $(|01\rangle_{1'2'} + |10\rangle_{1'2'})/\sqrt{2}$ in the case of $P_{1'2'}=0$. When $P_{1'2'}=1$, an additional σ_x operation is needed to apply on one of the output qubits.

Fig. 3 Controlled-phase gate on two logic-qubits in DFS, where logic-qubits are encoded in the pairs 1-2 and 5-6, and the two ancillary qubits 3 and 4 are measured at the exit of the circuit. H_L is from Fig. 2.

Table. 1 The corresponding rotation operation R_z for different values of P_1 and P_2 in the C-R block, where the case of $P_1=P_2=1$ is discussed in detail in appendix.

$P_2 \setminus P_1$	0	1
0	$R_z(\varphi) = e^{i(E_1\Delta t + \pi)}, R_z(\phi) = e^{i(E_1\Delta t' + \pi)}$	$R_z(\varphi) = e^{-i(E_1\Delta t - \pi)}, R_z(\phi) = e^{iE_1\Delta t'}$
1	$R_z(\varphi) = e^{iE_1\Delta t}, R_z(\phi) = e^{-i(E_1\Delta t' - \pi)}$	$R_z(\varphi) = e^{-iE_1\Delta t}, R_z(\phi) = e^{-iE_1\Delta t'}$

VI. APPENDIX

We present detailed derivation of Eq. (2) below, in which the relative phases due to free evolution of different levels will be fully considered. We set t_0 to be the time that physical-qubits 1 and $1'$ go into the circuit C-R. After a time Δt they reach the block P_1 , as shown in Fig. 1 (b), and the total system turns to,

$$\begin{aligned}
 |\Psi(t_0 + \Delta t)\rangle &= \frac{e^{i2E_1\Delta t}}{2} [\alpha(|0101\rangle_{121'2'} + |0110\rangle_{121'2'}) + \beta(|1001\rangle_{121'2'} + |1010\rangle_{121'2'})] \\
 &\quad \otimes (|0\rangle_a + |1\rangle_a e^{iE_1\Delta t}), \tag{A1}
 \end{aligned}$$

where we have assumed the energies of the states $|0\rangle$ and $|1\rangle$ to be, respectively, 0 and $-E_1$. The subscripts n ($n = 1, 2, 1', 2', a$) represent the corresponding physical-qubits. Qubits 1 and $1'$ are input from the control-in and target-in ports of the circuit C-R, respectively. Qubit a is input from the auxiliary port [See Fig. 1(b)]. Other two qubits, i.e., qubits 2 and $2'$ are idle at this stage. If we have $P_1 = 1$, the state of the system collapses into

$$\begin{aligned} |\Psi(t_0 + \Delta t)\rangle &= \frac{e^{i2E_1\Delta t}}{\sqrt{2}} [\alpha (|0101\rangle_{121'2'} |0\rangle_a + |0110\rangle_{121'2'} |0\rangle_a) \\ &+ \beta (|1001\rangle_{121'2'} |1\rangle_a e^{iE_1\Delta t} + |1010\rangle_{121'2'} |1\rangle_a e^{iE_1\Delta t})]. \end{aligned} \quad ((A2))$$

Then we perform Hadamard operation on the ancillary qubit during a time length $\Delta t'$, which yields,

$$\begin{aligned} |\Psi(t_0 + \Delta t + \Delta t')\rangle &= \frac{e^{i2E_1(\Delta t + \Delta t')}}{2} [\alpha |0101\rangle_{121'2'} (|0\rangle_a + |1\rangle_a e^{iE_1\Delta t'}) \\ &+ \alpha |0110\rangle_{121'2'} (|0\rangle_a + |1\rangle_a e^{iE_1\Delta t'}) \\ &+ \beta |1001\rangle_{121'2'} (|0\rangle_a e^{iE_1\Delta t} - |1\rangle_a e^{iE_1(\Delta t + \Delta t')}) \\ &+ \beta |1010\rangle_{121'2'} (|0\rangle_a e^{iE_1\Delta t} - |1\rangle_a e^{iE_1(\Delta t + \Delta t')})]. \end{aligned} \quad ((A3))$$

In the case of $P_2 = 1$, we have,

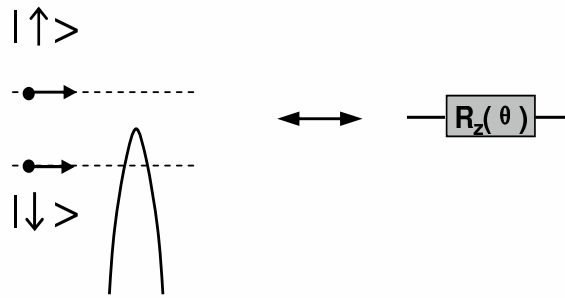
$$\begin{aligned} |\Psi(t_0 + \Delta t + \Delta t')\rangle &= \frac{e^{i2E_1(\Delta t + \Delta t')}}{2} [\alpha (|0101\rangle_{121'2'} |0\rangle_a + |0110\rangle_{121'2'} |1\rangle_a e^{iE_1\Delta t'}) \\ &+ \beta (|1001\rangle_{121'2'} |0\rangle_a e^{iE_1\Delta t} - |1010\rangle_{121'2'} |1\rangle_a e^{iE_1(\Delta t + \Delta t')})]. \end{aligned} \quad ((A4))$$

Then a measurement on the ancillary qubit in the dressed state $\{|+\rangle, |-\rangle\}$ leads to

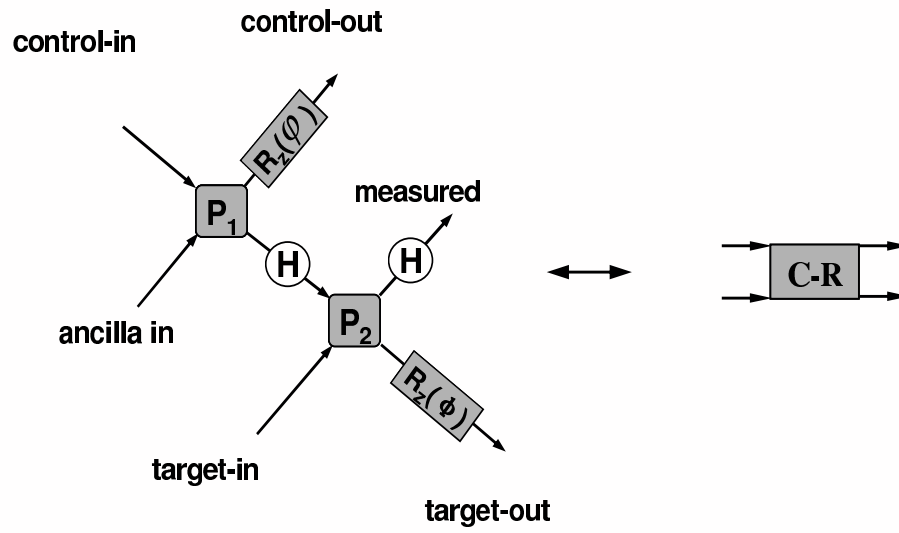
$$\alpha (|0101\rangle_{121'2'} + |0110\rangle_{121'2'} e^{iE_1\Delta t'}) + \beta (|1001\rangle_{121'2'} e^{iE_1\Delta t} - |1010\rangle_{121'2'} e^{iE_1(\Delta t + \Delta t')}), \quad ((A5))$$

in the case of the output $|+\rangle$. If the output is $|-\rangle$, an additional operation σ_z applied to qubit $1'$ is necessary. Assisted by single-qubit rotations $R_z(\varphi) = e^{-iE_1\Delta t}$ and $R_z(\phi) = e^{-iE_1\Delta t'}$, we could obtain Eq. (2). In fact, as shown in Eq. (A3), there is a possible leakage out of the DFS in the building blocks of the C-R operation in Fig. 1 (b). By a selective single-qubit rotations R_z in the building blocks, however, we can suppress this leakage, just like what is done by the 'Bang-Bang' pulse sequences introduced in [14, 15].

For different values of P_1 and P_2 , the deductions are similar and we can also reach Eq. (2) after different rotating phases by R_z , as shown in Table 1.



(a)



(b)

FIG. 1: Fig. 1

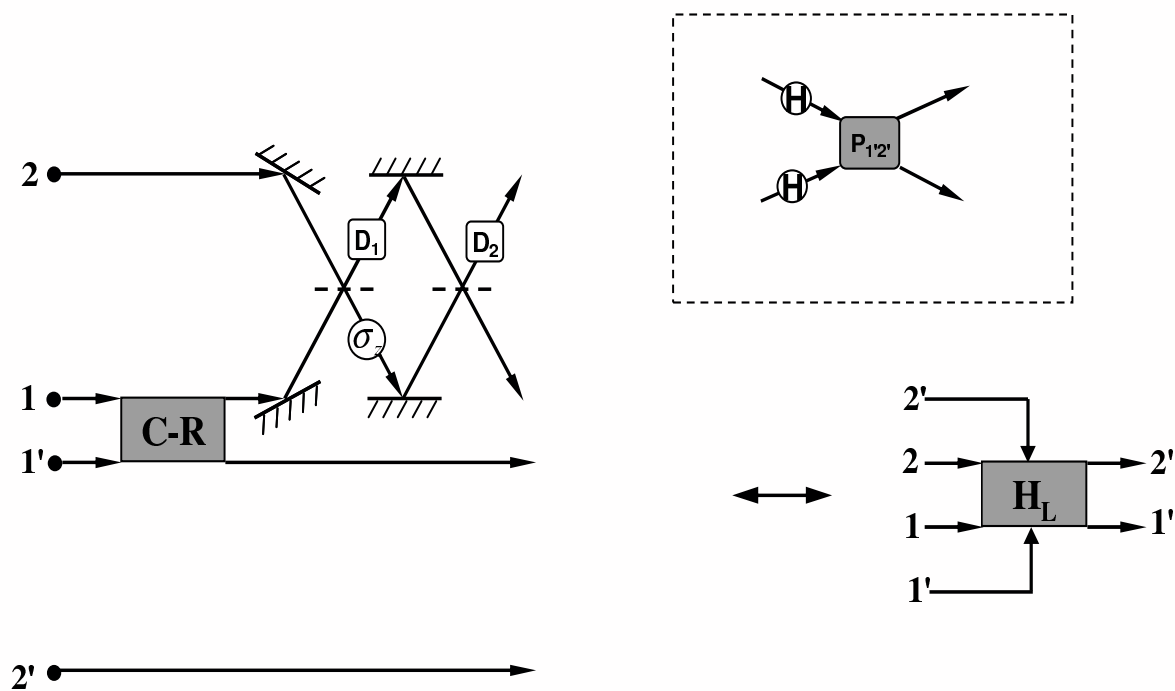


FIG. 2: Fig. 2

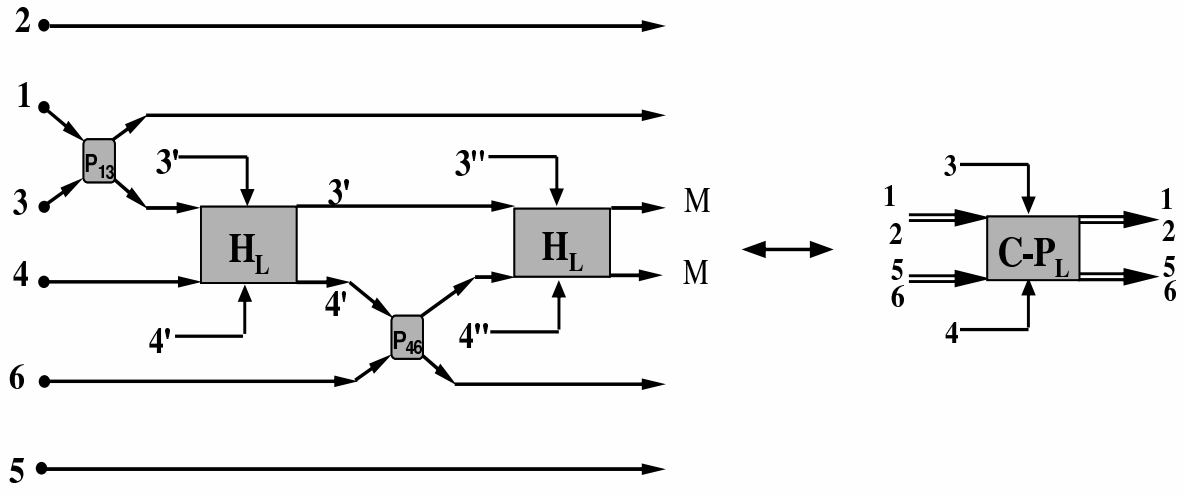


FIG. 3: Fig. 3